

Power computation for the triboelectric nanogenerator

J.H.B. Deane¹, R.D.I.G. Dharmasena² and G. Gentile³

¹Department of Mathematics, University of Surrey, Guildford, GU2 7XH, UK

²Advanced Technology Institute, University of Surrey, Guildford, GU2 7XH, UK

³Dipartimento di Matematica, Università Roma Tre, Roma, I-00146, Italy

Abstract

We consider, from a mathematical perspective, the power generated by a contact-mode triboelectric nanogenerator, an energy harvesting device that has been thoroughly studied recently. We encapsulate the behaviour of the device in a differential equation, which although linear and of first order, has periodic coefficients, leading to some interesting mathematical problems. In studying these, we derive approximate forms for the mean power generated and the current waveforms, and describe a procedure for computing the Fourier coefficients for the current, enabling us to compute the power accurately and show how the power is distributed over the harmonics. Comparisons with numerics validate our analysis.

1 Introduction

Triboelectric nanogenerators (TENGs) have received considerable attention recently as potential candidates for energy scavenging [1, 2, 3, 4]. These devices have been shown to convert mechanical energy into electricity in applications such as energy harvesting and self-powered sensors [5, 6, 7]. Furthermore, TENGs have many advantages over existing energy harvesting technologies [2, 3, 5, 7, 8], such as low cost, simple construction, relatively high power, flexibility and robustness.

The contact-mode triboelectric nanogenerator is the most commonly used TENG architecture owing to its simplicity and output performance [8, 9]. Typically, it consists of two triboelectric plates, at least one being of dielectric material, each attached to an electrode. When the plates come into contact, one becomes positively charged and the other, negatively. (Static electricity produced by friction is a well-known example of the same effect.) We feel that it is timely to discuss, from an applied mathematical point of view, the power produced by a TENG, whose construction is described in detail in for example [1, 4, 8].

A related device, a piezo-electric generator designed to harvest energy from the heartbeat, is described in [10], but its mathematical modelling, at least from the point of view we take here, is straightforward and so of less interest.

In this paper, we consider the most common configuration — two metal electrodes, each with a layer of dielectric attached — in order to assess its power output characteristics. Our starting point is the ordinary differential equation (o.d.e.) that describes such a TENG connected to a load resistance R . Our main assumption is that the TENG is being driven periodically at a frequency ω , that is to say, the separation of the plates varies periodically with time. We then adopt a circuit theory approach, as laid out in [11], by modelling the system as the circuit in Figure 1. The circuit leads directly to a differential equation, and this forms the basis for our study. The circuit and its mathematical

description are both straightforward, the only complication arising from the fact that the capacitance, $C(t)$, is a periodic function of time: this is inescapable and is a direct consequence of the periodically varying plate separation. It is this that generates the time variation in both the capacitance and the input voltage, and guarantees that their fundamental frequencies, ω , are identical.

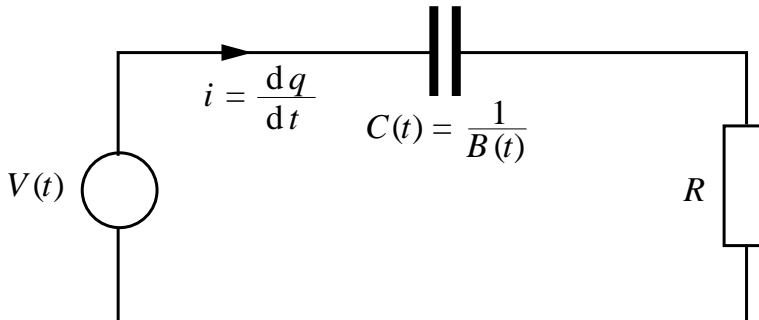


Figure 1: A circuit model of the TENG studied in this paper, in which the voltage source $V(t)$ and the capacitance $C(t)$ are both periodic with the same fundamental frequency ω . This circuit is described by the differential equation (2).

We are particularly interested in computing, both accurately and approximately, the mean power delivered to the load as a function of the parameters of the system, and in order to investigate this, we first take a perturbation theory approach. This leads to two formulae for the power, one valid for small R and the other for large R . We also tackle the same problem via Fourier series, this approach showing how the power generated is distributed over different harmonics, that is, integer multiples of ω . The mean (as opposed to, say, the peak) power is especially amenable to calculation, and is also the most appropriate measure of the effectiveness of the generator.

We should give here some justification for our analytical approach, which takes up the bulk of the paper. After all, the mean power, current waveforms and so on can also be computed numerically — why, then, compute them analytically? We offer several reasons for our approach. In general, analytical results give deeper insight into the problem, and in this paper, we derive several approximate expressions for the variables of interest, and use these, for instance, to optimise the power output by means of simple arguments. For example, we derive, by perturbation theory, a simple expression for the value of R that maximises the mean power. Contrast this with a purely numerical approach, in which such an optimisation would have to be carried out for one set of parameters at a time. Furthermore, for large R , the transient times are large — a numerical solution would have to be continued for long times in order to ensure that the transient has decayed sufficiently. By contrast, our analytical solution is set up specifically to correspond to the steady state (post-transient) behaviour. The Fourier series approach, which we also discuss, immediately gives insight into how rapidly the Fourier coefficients decrease in magnitude with index. It also turns out to be possible to express these coefficients explicitly in terms of Bessel functions.

The rest of the paper is organised as follows. We first derive the o.d.e., including the periodic functions $V(t)$ and the reciprocal capacitance (elastance), $B(t) := 1/C(t)$. Both of these depend on a function $I(x)$, which in turn comes from calculating the electric field in the system. This was derived in [1] for square plates; for the sake of completeness, we give the derivation in the slightly more general case of rectangular plates in Appendix I. On examining both $V(t)$ and $B(t)$ for practical values of the parameters, we make simple approximations to them, which in turn leads to a simplified

version of the o.d.e. We then carry out the mean power calculations mentioned above, in both the case of general periodic source voltage and elastance, and their approximations, and follow this with some comparisons between numerical solutions of the o.d.e. in both cases. This comparison shows the approximations to be very good. We then discuss an approach to power computation based on Fourier series, after which we draw some conclusions.

2 The o.d.e.

The o.d.e. in its original form

$$AR\dot{\sigma} + \underbrace{\frac{1}{\pi} \left(\frac{1}{\epsilon_1} + \frac{1}{\epsilon_2} \right) \{I(x_1 + x_2 + z(t)) - I_0\}}_{G(t)} \sigma = F_1(t) + F_2(t) \quad (1)$$

was discussed in [1]. Here, $\sigma(t)$, to be solved for, is the surface charge density and $\dot{\sigma}$ is its time derivative. Also, $A = wl = \alpha w^2$ is the area of the plates, $\alpha = l/w$ is their aspect ratio, $R > 0$ is a fixed load resistance, ϵ_1 and ϵ_2 are the permittivities of the dielectrics, with thickness x_1 and x_2 respectively; and σ_T is the triboelectric charge density, which is constant and a property of the materials used. Furthermore, the excitation $z(t) = z_0[1 + \sin(\omega t + \phi)]$, where z_0 is the amplitude, ϕ is a fixed phase angle, and $\omega = 2\pi f$ is the excitation frequency; and $F_i = \frac{\sigma_T}{\pi\epsilon_i} \{I(x_i + z(t)) - I(x_i)\}$, with $i = 1, 2$, where $I(x)$ is defined in equation (28) in Appendix I. Finally, $I_0 = \lim_{x \rightarrow 0} I(x)$. The variable parameters of interest are R and ω — we consider all the other parameters to be fixed.

Since σ is a charge density, we interpret $q := A\sigma$ as a charge. Hence, replacing $A\sigma$ in equation (1) with q , we have

$$R\dot{q} + \frac{G(t)}{A}q = F_1(t) + F_2(t),$$

where $G(t)$ is defined in equation (1); and it becomes clear that the function of time that multiplies q can be interpreted as the reciprocal of a time-dependent capacitance, provided that this is defined as the ratio of the change in the charge in the system to the change in potential difference (as opposed to the derivative of the charge with respect to potential difference); and that the term on the right hand side is a time-dependent voltage, $V(t) = F_1(t) + F_2(t)$. That is,

$$R\dot{q} + B(t)q = V(t) \quad (2)$$

where

$$B(t) = \frac{G(t)}{A} = \frac{1}{A\pi} \left(\frac{1}{\epsilon_1} + \frac{1}{\epsilon_2} \right) \{I(x_1 + x_2 + z(t)) - I_0\}. \quad (3)$$

We claim that equation (2) models the TENG and the rest of this paper discusses its periodic solution, $q(t)$, from which the current, $i(t) := \dot{q}(t)$, and much else, can be deduced.

2.1 Practical parameter values

Typical values for the parameters, taken from [1], are given in Table 1. Plots of the exact $C(t)$, $B(t)$ and $V(t)$ are given in Figure 2 for these parameter values. Note that, despite the fact that $z(t)$ contains only one harmonic, $C(t)$ and $V(t)$ contain all harmonics owing to the nonlinear function $I(\text{const.} + z(t))$ used in their definition. However, Figure 2 suggests that a good approximation might be obtained by only considering the first harmonic.

Parameter values for practical triboelectric nanogenerator		
Name	Symbol	Numerical value
Permittivity of free space	ϵ_0	$8.854 \times 10^{-12} \text{ Fm}^{-1}$
Permittivity of dielectric 1	ϵ_1	$3.30\epsilon_0$
Permittivity of dielectric 2	ϵ_2	$3.27\epsilon_0$
Triboelectric charge density	σ_T	$4.8 \times 10^{-5} \text{ Cm}^{-2}$
Thickness of dielectric 1	x_1	$200 \text{ }\mu\text{m}$
Thickness of dielectric 2	x_2	$20 \text{ }\mu\text{m}$
Default aspect ratio, l/w	α	1
Default plate dimensions	l, w	$l = w = 5 \times 10^{-2} \text{ m}$
Default plate area	A	$2.5 \times 10^{-3} \text{ m}^2$
Excitation amplitude & phase	z_0, ϕ	resp. $1.0 \times 10^{-3} \text{ m}$, $3\pi/2$
Elastance parameters	B_0, B_1	resp. 1.6×10^{10} , $1.3 \times 10^{10} \text{ F}^{-1}$
Drive voltage amplitude	V_0	1550 V
Excitation frequency	$f = \omega/2\pi$	$0.1 - 10^3 \text{ Hz}$ (nom. 1 Hz)
Load resistance	R	$10^5 - 10^{15} \Omega$

Table 1: Names, symbols and numerical values for the parameters for a practical TENG. Note the very large range of the parameter R .

2.2 The practical approximation

Clearly, $I(\text{constant} + z(t))$ is not sinusoidal, even though $z(t)$ is: so strictly speaking, $B(t)$ and $V(t)$ should be expanded as Fourier series, both with identical fundamental frequency ω . However, in the practical case considered here, x_1 , x_2 , z_0 and I are such that good first approximations for $B(t)$ and $V(t)$ are

$$B(t) = \sum_{k \in \mathbb{Z}} b_k e^{ik\omega t} \approx B_0 - B_1 \cos \omega t \quad V(t) = \sum_{k \in \mathbb{Z}} v_k e^{ik\omega t} \approx V_0(1 - \cos \omega t), \quad (4)$$

as suggested by Figure 2. In fact, $|b_2/b_1| \approx 9.385 \times 10^{-3}$, $|b_3/b_1| \approx 7.610 \times 10^{-6}$ and $|v_2/v_1| \approx 9.351 \times 10^{-3}$, $|v_3/v_1| \approx 6.898 \times 10^{-6}$. Thus, we study where appropriate both the general o.d.e. with

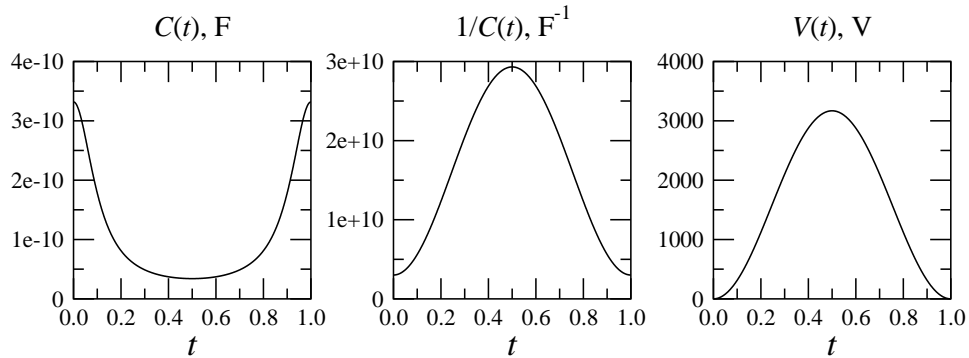


Figure 2: The periodic functions of time in equation (2), for $\omega = 2\pi \text{ rad/s}$: $C(t)$, left; $B(t) = 1/C(t)$, middle; and $V(t)$, right. None of the functions are approximated. Parameter values are from Table 1.

$B(t)$ and $V(t)$ subject to some mild conditions but otherwise arbitrary, and also the approximate o.d.e.

$$R\dot{q} + (B_0 - B_1 \cos \omega t)q = V_0(1 - \cos \omega t). \quad (5)$$

We refer to equation (5) as the ‘practical approximation’ in what follows. A better approximation would take into account more terms in the Fourier series expansions of $B(t)$ and $V(t)$, but in practice, for the parameter values given in Table 1, this approximation gives good results — as we shall see.

3 Analytical results

3.1 Unique periodic attractor

In this section, we show that, under conditions that must apply on physical grounds, there is a unique periodic solution to the differential equation (2), and that solutions starting from any initial condition are attracted to it. We can then talk about ‘the periodic solution’, knowing that this exists.

In a real system described by the differential equation (2), on physical grounds alone, $B(t)$ and $V(t)$ must satisfy the Dirichlet conditions [12], and so both functions can be expanded in Fourier series. Furthermore, as shown in the Appendix I, $B(t) > 0$ for all t and so the mean value of $B(t) > 0$. We will use both these facts in what follows.

In practice, we will be interested only in periodic solutions to the o.d.e. (2), but in this section alone, we need to solve the o.d.e. for the complete solution, which we call $q_c(t)$. The standard way to solve such an o.d.e. is by the integrating factor method [13], which gives

$$q_c(t) = \exp \left\{ -\frac{1}{R} \int_0^t B(t') dt' \right\} \left[\frac{1}{R} \int_0^t V(t') \exp \left\{ \frac{1}{R} \int_0^{t'} B(t'') dt'' \right\} dt' + q_c(0) \right]. \quad (6)$$

Although the solution in this form is not obviously useful for direct computation of, for instance, the mean power, it *is* useful to show that for any initial condition, $q_c(0)$, there is a unique periodic attractor. We now prove this.

We introduce the notation for the mean, $\langle f \rangle$, of any periodic function $f(t)$ with period T_0 , which is

$$\langle f \rangle := \frac{1}{T_0} \int_{-T_0/2}^{T_0/2} f(t) dt.$$

We then define $\tilde{f}(t) := f(t) - \langle f \rangle$ as the zero-mean, time-varying part of $f(t)$.

Since $B(t)$ and $V(t)$ both have the same period $T_0 = 2\pi/\omega$, all the time-varying terms in equation (6) have period T_0 . Hence, writing $B(t) = \langle B \rangle + \tilde{B}(t)$, we can make the following Fourier expansion:

$$\frac{V(t)}{R} \exp \left\{ \frac{1}{R} \int_0^t B(t') dt' \right\} = e^{\langle B \rangle t / R} \frac{V(t)}{R} \exp \left\{ \frac{1}{R} \int_0^t \tilde{B}(t') dt' \right\} = e^{t/\tau} \sum_{k \in \mathbb{Z}} I_k e^{ik\omega t},$$

where $\tau = R/\langle B \rangle > 0$ since both R and $\langle B \rangle$ are positive, and Fourier coefficients $I_k \in \mathbb{C}$ have dimensions of current. Using this in (6) then gives

$$\begin{aligned} q_c(t) &= e^{-t/\tau} \exp \left\{ -\frac{1}{R} \int_0^t \tilde{B}(t') dt' \right\} \left[\int_0^t \sum_{k \in \mathbb{Z}} I_k e^{(1+ik\omega\tau)t'/\tau} dt' + q_c(0) \right] \\ &= \exp \left\{ -\frac{1}{R} \int_0^t \tilde{B}(t') dt' \right\} \left[\sum_{k \in \mathbb{Z}} \frac{\tau I_k e^{ik\omega t}}{1 + ik\omega\tau} + e^{-t/\tau} \left(q_c(0) - \sum_{k \in \mathbb{Z}} \frac{\tau I_k}{1 + ik\omega\tau} \right) \right]. \end{aligned}$$

From this we deduce that

1. Since $\tau > 0$, as $t \rightarrow \infty$, for all initial conditions $q_c(0)$, $q_c(t)$ tends to the period- T_0 function

$$q(t) = \exp \left\{ -\frac{1}{R} \int_0^t \tilde{B}(t') dt' \right\} \sum_{k \in \mathbb{Z}} \frac{\tau I_k e^{ik\omega t}}{1 + ik\omega\tau};$$

2. Any solution $q_c(t)$ approaches this periodic attractor exponentially,¹ that is, $|q_c(t) - q(t)| < ce^{-t/\tau}$ for some positive constant c .
3. The choice $q_c(0) = \sum_{k \in \mathbb{Z}} \tau I_k / (1 + ik\omega\tau)$ puts the solution directly on the periodic attractor.

3.2 Perturbation series — small R

Although the previous section derives an exact expression for the complete solution, $q_c(t)$, and the periodic solution, $q(t)$, these expressions do not lend themselves to direct computation of the power, or simple approximations to it. To circumvent this, we estimate $q(t)$ using a perturbation theory approach. Underlying this approach is the assumption that $B(t)$ and $V(t)$ are both infinitely differentiable (which is clearly the case for the practical approximation).

Our starting point is to define the dimensionless parameter $\varepsilon := \omega R / \langle B \rangle$, which is small for small R . In terms of this, we re-write the o.d.e. (2) as

$$\varepsilon \dot{q} + \frac{\omega}{\langle B \rangle} B(t) q = \frac{\omega}{\langle B \rangle} V(t). \quad (7)$$

We now set

$$q(t) = q_0(t) + \varepsilon q_1(t) + \varepsilon^2 q_2(t) + \dots, \quad (8)$$

and substituting this into (7), and equating to zero the coefficients of each power of ε , we find

$$\varepsilon^0: q_0 = \frac{V}{B}, \quad \varepsilon^1: \dot{q}_0 + \frac{\omega}{\langle B \rangle} B q_1 = 0, \quad \varepsilon^2: \dot{q}_1 + \frac{\omega}{\langle B \rangle} B q_2 = 0, \dots, \quad \varepsilon^k: \dot{q}_{k-1} + \frac{\omega}{\langle B \rangle} B q_k = 0,$$

where for brevity we have dropped the argument (t) for B , V and q_k . Hence, we have

$$q_0 = \frac{V}{B}, \quad q_1 = -\frac{\langle B \rangle}{\omega B} \frac{d}{dt} \left(\frac{V}{B} \right) = -\frac{\langle B \rangle}{\omega} \frac{B\dot{V} - \dot{B}V}{B^3},$$

$$q_2 = -\frac{\langle B \rangle}{\omega B} \dot{q}_1 = \frac{\langle B \rangle^2}{\omega^2} \frac{1}{B} \frac{d}{dt} \left(\frac{1}{B} \frac{d}{dt} \left(\frac{V}{B} \right) \right) = \frac{\langle B \rangle^2}{\omega^2} \frac{B(B\ddot{V} - \ddot{B}V) - 3\dot{B}(B\dot{V} - \dot{B}V)}{B^5}$$

with obvious generalisations for q_k , $k > 2$. The above expressions for q_k are general, in that they apply for any infinitely differentiable functions B, V provided only that $B > 0$, $\forall t$.

The power series expansion (8) is very unlikely to converge. Even in the case of constant B , it is easy to check that the periodic solution $q(t)$ is not analytic around $\varepsilon = 0$ for a generic, analytic $V(t)$ containing all the harmonics. Additionally, the presence of the function $B(t)$ will only complicate the situation. However, even though the series expansion is not expected to be convergent, it is likely to

¹Although the rate of approach to the attractor will be very slow for large R (i.e. large τ).

be an asymptotic series, and hence any truncation of it should provide a reliable approximation of the full solution, for ε small enough.

We can make further progress from this point if we use the practical approximation, which is that $B(t) = B_0 - B_1 \cos \omega t$ and $V(t) = V_0(1 - \cos \omega t)$, where $B_0 = \langle B \rangle > B_1 > 0$. With these definitions of B and V in force, we have that, for $k \in \mathbb{N}$, q_{2k-1} are odd and q_{2k} are even functions of t ; hence, \dot{q}_{2k-1} are even and \dot{q}_{2k} are odd. The instantaneous power $p(t) := \dot{q}(t)^2 R$ and the mean power is defined as $\langle p \rangle := \langle \dot{q}^2 \rangle R$. From the perturbation series (8), we have

$$\langle \dot{q}^2 \rangle = \langle \dot{q}_0^2 \rangle + 2\varepsilon \langle \dot{q}_0 \dot{q}_1 \rangle + \varepsilon^2 (2 \langle \dot{q}_0 \dot{q}_2 \rangle + \langle \dot{q}_1^2 \rangle) + O(\varepsilon^3).$$

Now, by the definition of $\langle f \rangle$ we have that $\langle f \rangle = 0$ if f is an odd function of t . Thus, using the parity of functions q_k and their first derivatives, we have that $\langle \dot{q}_0 \dot{q}_1 \rangle = 0$ and so on. Hence, for small R , and so for small ε , we have

$$\langle p \rangle_s = R \langle \dot{q}_0^2 \rangle + R \varepsilon^2 (2 \langle \dot{q}_0 \dot{q}_2 \rangle + \langle \dot{q}_1^2 \rangle) + O(\varepsilon^4).$$

Since it is useful to know the dependence of $\langle p \rangle$ on ω as well as R , we compute

$$\langle \dot{q}_0^2 \rangle = \frac{1}{T_0} \int_{-T_0/2}^{T_0/2} \frac{(B\dot{V} - \dot{B}V)^2}{B^4} dt = \frac{\omega^2}{2\pi} \int_{-\pi}^{\pi} \frac{(BV' - B'V)^2}{B^4} dx := \omega^2 a_1,$$

where we have substituted $x = \omega t$ and used a prime to denote differentiation with respect to x . In fact, this integral can be evaluated in closed form; it is

$$a_1 = \frac{V_0^2 B_0}{2\sqrt{B_0^2 - B_1^2}(B_0 + B_1)^2}. \quad (9)$$

From our previous definitions of q_0 , q_1 and q_2 , we also have

$$\frac{2}{\omega^2 B_0^2} \langle \dot{q}_0 \dot{q}_2 \rangle = \frac{1}{\pi} \int_{-\pi}^{\pi} \left(\frac{V}{B} \right)' \frac{d}{dx} \left\{ \frac{1}{B} \frac{d}{dx} \left[\frac{1}{B} \left(\frac{V}{B} \right)' \right] \right\} dx$$

and

$$\frac{1}{\omega^2 B_0^2} \langle \dot{q}_1^2 \rangle = \frac{1}{2\pi} \int_{-\pi}^{\pi} \left\{ \frac{d}{dx} \left[\frac{1}{B} \left(\frac{V}{B} \right)' \right] \right\}^2 dx.$$

Defining a_3 as the sum of the right hand sides of these two expressions, we can also determine that

$$a_3 = \frac{V_0^2 B_0 (8B_0^4 + 44B_0^2 B_1^2 + 17B_1^4)}{16\sqrt{B_0^2 - B_1^2}(B_0 - B_1)^3(B_0 + B_1)^5}.$$

Bearing in mind now that $\varepsilon = \omega R/B_0$, and that a_1, a_3 do not depend on ω or R , we have that

$$\begin{aligned} \langle p \rangle_s &= a_1 \omega^2 R + a_3 \omega^4 R^3 + O(\omega^6 R^5) \\ &= 2.45018 \times 10^{-15} \omega^2 R - 1.35505 \times 10^{-33} \omega^4 R^3 + O(\omega^6 R^5) \end{aligned} \quad (10)$$

where a_1 and a_3 have been evaluated using the values in Table 1.

3.3 Perturbation series — large R

In the case of large R , we compute a solution to the o.d.e. in a similar way to the previous section, this time expanding as a power series in the dimensionless, small parameter $\delta := \langle B \rangle / \omega R (= 1/\varepsilon)$. In terms of δ , the o.d.e. (2) becomes

$$\dot{q} = \delta \frac{\omega}{\langle B \rangle} [V(t) - q B(t)]. \quad (11)$$

Again, we expand $q(t) = q_0(t) + \delta q_1(t) + \delta^2 q_2(t) + \delta^3 q_3(t) + \dots$ and, substituting this into (11) and matching powers of δ , we find

$$\delta^0 : \quad \dot{q}_0 = 0, \quad \delta^1 : \quad \dot{q}_1 = \frac{\omega}{\langle B \rangle} (V - q_0 B), \quad \delta^2 : \quad \dot{q}_2 = -\frac{\omega}{\langle B \rangle} B q_1, \quad \delta^3 : \quad \dot{q}_3 = -\frac{\omega}{\langle B \rangle} B q_2$$

and so on.

The guiding principle for finding q_k is that for each k , q_k is periodic. Hence, when q_k is expressed as an integral, we must ensure that the integrand has, in each case, zero mean (otherwise the integral will grow linearly with t).

The equation $\dot{q}_0 = 0$ has solution $q_0 = c_0$ for c_0 an as yet undetermined constant. Hence, we have $\dot{q}_1 = \omega(V - c_0 B)/\langle B \rangle$. Recalling that $B(t) = \langle B \rangle + \tilde{B}(t)$ and $V(t) = \langle V \rangle + \tilde{V}(t)$, we find

$$q_1(t) = \frac{\omega}{\langle B \rangle} \int_0^t \langle V \rangle - c_0 \langle B \rangle + \tilde{V}(t') - c_0 \tilde{B}(t') dt' + c_1,$$

where c_1 is a constant to be determined at the next stage. Furthermore, in order for the integrand here to have zero mean, we require $c_0 = \langle V \rangle / \langle B \rangle$. Hence,

$$q_1(t) = \frac{\omega}{\langle B \rangle^2} \int_0^t \langle B \rangle \tilde{V}(t') - \langle V \rangle \tilde{B}(t') dt' + c_1 \quad \text{and} \quad \dot{q}_1(t) = \frac{\omega}{\langle B \rangle^2} \left(\langle B \rangle \tilde{V}(t) - \langle V \rangle \tilde{B}(t) \right).$$

The constant c_1 is found in an analogous way to c_0 . Since $\dot{q}_2(t) = -\omega B(t)q_1(t)/\langle B \rangle$, we have, using our expression for $q_1(t)$,

$$q_2(t) = -\frac{\omega}{\langle B \rangle} \int_0^t \left(\langle B \rangle + \tilde{B}(t') \right) \left\{ \int_0^{t'} \frac{\omega}{\langle B \rangle^2} \left(\langle B \rangle \tilde{V}(t'') - \langle V \rangle \tilde{B}(t'') \right) dt'' + c_1 \right\} dt' + c_2, \quad (12)$$

where c_2 is a new constant that can be determined at the next stage. Reasoning as before, for $q_2(t)$ to be periodic, the integrand of the integral w.r.t. t' in equation (12) must have mean zero, which fixes c_1 by

$$c_1 = -\frac{\omega^2}{2\pi \langle B \rangle^3} \int_{-T_0/2}^{T_0/2} \left(\langle B \rangle + \tilde{B}(t') \right) \left\{ \int_0^{t'} \left(\langle B \rangle \tilde{V}(t'') - \langle V \rangle \tilde{B}(t'') \right) dt'' \right\} dt'.$$

We can in principle continue in the same way to find q_k , $k > 2$.

Using the practical approximation for $B(t)$ and $V(t)$, we find $q_0 = V_0/B_0$, $c_1 = 0$ and so

$$q_1(t) = -\frac{V_0(B_0 - B_1)}{B_0^2} \sin \omega t, \quad q_2(t) = \frac{V_0(B_0 - B_1)}{4B_0^3} (B_1 \cos 2\omega t - 4B_0 \cos \omega t + 4B_0 - B_1) + c_2.$$

In what follows, we also need an expression for \dot{q}_3 , which obeys $\dot{q}_3 = -\omega B(t)q_2(t)/B_0$. Hence, we require a value for c_2 , which we again deduce by imposing the condition that

$$q_3 = -\frac{\omega}{B_0} \int_0^t (B_0 - B_1 \cos \omega t') \{K_1 (B_1 \cos 2\omega t' - 4B_0 \cos \omega t' + 4B_0 - B_1) + c_2\} dt' + c_3,$$

where $K_1 = V_0(B_0 - B_1)/4B_0^3$, is bounded as $t \rightarrow \infty$. Since $\langle \cos \omega t \rangle = \langle \cos \omega t \cos 2\omega t \rangle = 0$ but $\langle \cos^2 \omega t \rangle = 1/2$, this condition gives

$$c_2 = -\frac{V_0(B_0 - B_1)(4B_0 + B_1)}{4B_0^3}$$

and so

$$q_3(t) = \frac{V_0(B_0 - B_1)}{24B_0^4} (3(8B_0^2 - 3B_1^2) \sin \omega t - 9B_0B_1 \sin 2\omega t + B_1^2 \sin 3\omega t) + c_3.$$

To find the mean power, we again need to compute $\langle \dot{q} \rangle^2 = \delta^2 \langle \dot{q}_1^2 \rangle + \delta^3 \langle \dot{q}_1 \dot{q}_2 \rangle + \delta^4 \langle 2\dot{q}_1 \dot{q}_3 + \dot{q}_2^2 \rangle + O(\delta^6)$, where, as before, we observe that $\dot{q}_1(t)\dot{q}_2(t)$ is an odd function of t in the practical approximation, so its mean is zero. From the above expressions for q_1, q_2, q_3 , we find

$$\langle \dot{q}_1^2 \rangle = \frac{1}{2} \left(\frac{V_0(B_0 - B_1)}{B_0^2} \right)^2 \omega^2, \quad \langle 2\dot{q}_1 \dot{q}_3 + \dot{q}_2^2 \rangle = -\frac{V_0^2(B_0 - B_1)^3(B_0 + B_1)}{2B_0^6} \omega^2.$$

Defining the mean power for large R , $\langle p \rangle_l$, as $\langle p \rangle_l := R \langle \dot{q}^2 \rangle$ we have

$$\begin{aligned} \langle p \rangle_l &= \frac{1}{2} \left(\frac{V_0(B_0 - B_1)}{B_0} \right)^2 R^{-1} - \frac{V_0^2(B_0 - B_1)^3(B_0 + B_1)}{2B_0^2} \omega^{-2} R^{-3} + O(\omega^{-4} R^{-5}) \\ &= 42231.4 R^{-1} - 3.67414 \times 10^{24} \omega^{-2} R^{-3} + O(\omega^{-4} R^{-5}) \end{aligned} \quad (13)$$

where we have used the parameter values in Table 1 to obtain the last expression.

3.4 Comparison with numerics

We now make two comparisons. The first, in Figure 3, is a plot of the mean power, computed in four different ways:

- By solving the o.d.e. (2) numerically, using a good numerical algorithm (the Livermore Stiff o.d.e. solver [14]), with the value of $q(0)$ computed by Fourier series, using (a) the approximate $B(t), V(t)$ functions (circles in Figure 3) and (b) the exact expressions for them (crosses);
- By perturbation theory, as derived in the previous two subsections, with the dashed line showing $\langle p \rangle_s$ for $R \in [10^5, 10^8]$, as given by equation (10), and the continuous line, $\langle p \rangle_l$ from equation (13), for $R \in [3 \times 10^9, 10^{15}]$.

The agreement between approximate and exact B, V is seen to be very good, as are the perturbation expressions (within their ranges of applicability).

The second comparison is between currents, computed numerically using the exact $B(t), V(t)$, and from perturbation theory up to and including the terms $\dot{q}_3(t)$, both in the small and large R cases (\dot{q}_3 is only needed for large R). See Figure 4, which compares the numerical solution with the small R perturbation solution ($R = 10^7 \Omega$) and with the large R perturbation solution ($R = 10^{10} \Omega$). The two curves are almost exactly superimposed.

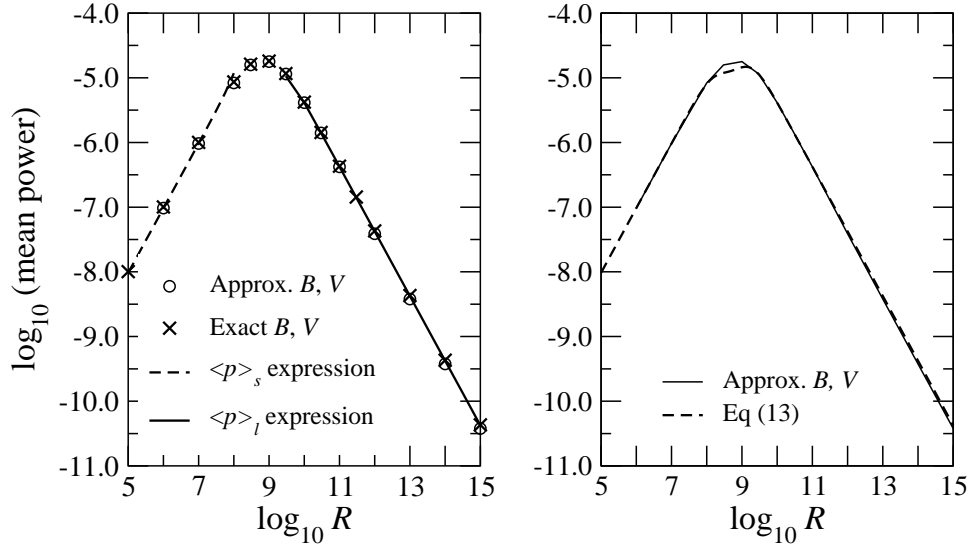


Figure 3: Left: The mean power, computed directly from a numerically-obtained $i(t) = \dot{q}(t)$ waveform and not from Fourier series, versus R , using the approximate (circles) and exact (crosses) expressions for $B(t)$ and $V(t)$. Also shown, over appropriately restricted ranges of R , are the series/asymptotic expansions for $\langle p \rangle_s$ and $\langle p \rangle_l$, from equations (10) and (13) respectively. Right — see section 3.6: mean power from the numerical $i(t)$ as in the left-hand figure with approximate B, V , (solid line), and also using the rational approximation $\langle p(R) \rangle$, equation (15) (dashed line).

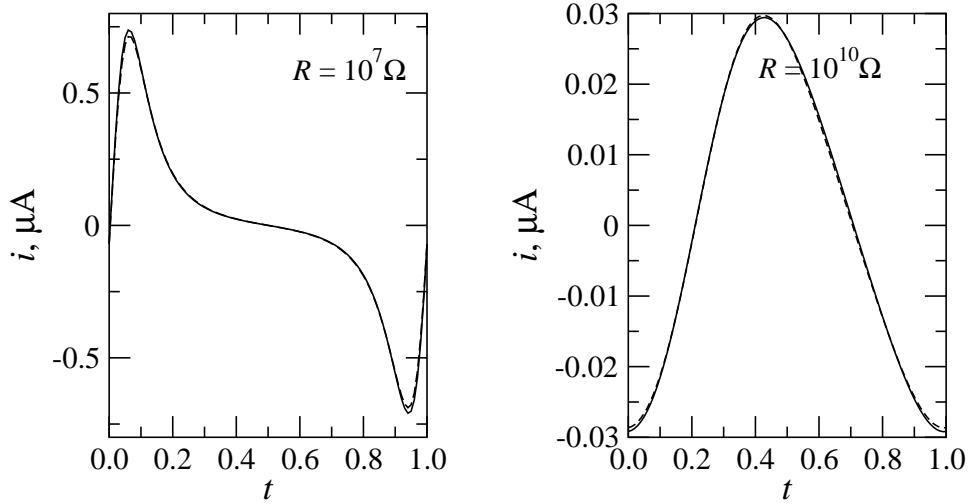


Figure 4: The current, computed by solving the o.d.e. (2) numerically (continuous lines) and using the perturbation series (dashed lines). On the left, $R = 10^7 \Omega$ and the small R series is used; on the right, $R = 10^{10} \Omega$ and the large R series is used. The curves are sufficiently close that they are almost indistinguishable.

3.5 Applications of the perturbation solutions

We now briefly discuss some applications of equations (10) and (13), the mean power expressions for small and large R respectively.

In general, these expressions between them give a good approximation to $\langle p \rangle$, in a very simple form, for all R except $10^8 \leq R \leq 3 \times 10^9$, and this may in itself be useful. Furthermore, we have derived expressions for $q(t)$ up to $O(\varepsilon^2)$ for small R and $O(\delta^3)$ for large R , where $\varepsilon = \omega R / \langle B \rangle$ and $\delta = 1/\varepsilon$. These approximations are good, as can be seen from Figure 4.

Less obviously, the perturbation series can also be used to estimate R_{pk} , the value of R for which the peak mean power is obtained. Taking logarithms, and only including the first terms of equations (10) and (13) respectively, we find

$$\ln \langle p \rangle = \ln (a_1 \omega^2 R) + O(R^2) \quad \text{and} \quad \ln \langle p \rangle = \ln (b_1 R^{-1}) + O(R^{-2}),$$

where a_1 and b_1 are given in (9) and (13) respectively. On a plot of $\ln \langle p \rangle$ versus $\ln R$, these are straight lines, and their intersection point gives an estimate of R_{pk} . This is

$$R_{pk} \approx \frac{1}{\omega} \sqrt{\frac{b_1}{a_1}} = \frac{B_0}{\omega} \left(1 - \frac{B_1^2}{B_0^2} \right)^{5/4} = \frac{4.152}{\omega} \text{ G}\Omega. \quad (14)$$

We postpone discussion of the accuracy of this until we have a more accurate computation of R_{pk} at the end of section 4.1. Note that this argument will always overestimate the power, however.

3.6 Mean power for all R ?

We end this section with an observation. Clearly, it would be useful to have a simple formula for the mean power, $\langle p(R) \rangle$, valid for *all* R , rather than the restricted ranges accessible via perturbation theory. A heuristic approach yields a non-rigorous result, which we now briefly discuss.

Looking at equations (10) and (13) suggests that these expressions might be, respectively, the Maclaurin series and an asymptotic expansion of a single odd function of ωR

$$\omega F(\omega R) = \omega \frac{A_1 \cdot \omega R + A_3 \cdot \omega^3 R^3}{1 + B_2 \cdot \omega^2 R^2 + B_4 \cdot \omega^4 R^4},$$

where A_1 , A_3 , B_2 and B_4 are constants to be found. By definition, this function is a candidate for $\langle p(R) \rangle$. In fact, all F does is to interpolate smoothly between the small and large R regimes; how it behaves for intermediate values of R is beyond our control.

Expanding $\omega F(\omega R)$ in a Maclaurin series, we find

$$\langle p \rangle_s = A_1 \omega^2 R + (A_3 - A_1 B_2) \omega^4 R^3 + O(\omega^6 R^5)$$

whereas the asymptotic expansion, that is, the Maclaurin series for $\omega F(\frac{1}{\omega R})$ in powers of $\frac{1}{\omega R}$, is

$$\langle p \rangle_l = \frac{A_3}{B_4} \frac{1}{R} + \frac{A_1 B_4 - A_3 B_2}{B_4^2} \frac{1}{\omega^2 R^3} + O(\omega^{-4} R^{-5}).$$

Matching the coefficients of the various powers of R with equations (10) and (13) gives four equations to solve for A_1 , A_3 , B_2 and B_4 , and doing so gives

$$\omega F(\omega R) = \omega^2 R \frac{2.45018 \times 10^{-15} + 2.99655 \times 10^{-34} \omega^2 R^2}{1 + 6.75329 \times 10^{-19} \omega^2 R^2 + 7.09553 \times 10^{-39} \omega^4 R^4} \stackrel{?}{=} \langle p(R) \rangle. \quad (15)$$

Figure 3, right-hand side, shows a comparison between $\langle p(R) \rangle$ approximated in this way, and a numerical computation. Solving $\partial \langle p(R) \rangle / \partial R = 0$ for R gives one positive, one negative and four complex values of R . The positive one is $R_{max} = 8.09 \times 10^9 / \omega = 1.29 \times 10^9 \Omega$ for $\omega = 2\pi$, and $\langle p(R_{max}) \rangle = 15.2 \mu\text{W}$. Compare these with the numerical computation in Figure 3, which gives $R_{max} = 6.8 \times 10^8 \Omega$ and $\langle p(R_{max}) \rangle = 18.2 \mu\text{W}$.

4 A Fourier series approach

An alternative approach to computing $q(t)$ is to use Fourier series: having established in section 3.1 that there is a unique attracting periodic solution, the idea here is to expand it as a Fourier series. In this section, we use the practical approximation for $B(t)$ and $V(t)$, although the ideas could be applied for any B, V of the same period. We start by setting

$$q(t) = \sum_{k \in \mathbb{Z}} \alpha_k e^{ik\omega t}, \quad (16)$$

where $\alpha_k \in \mathbb{C}$, with $\alpha_{-k} = \alpha_k^*$, so $\alpha_0 \in \mathbb{R}$, as is $q(t)$ for real t . Substituting this in the o.d.e., we find that the α_k must obey the following relations:

$$\alpha_1 = \eta\alpha_0 - \alpha_{-1} - 2Q_0, \quad (17a)$$

$$\alpha_2 = \eta(1 + i\varepsilon)\alpha_1 - \alpha_0 + Q_0, \quad (17b)$$

$$\alpha_{k+1} = \eta(1 + i\varepsilon k)\alpha_k - \alpha_{k-1}, \quad |k| \geq 2, \quad (17c)$$

where we have used the dimensionless real parameters $\varepsilon = \omega R / B_0$, as before, and $\eta := 2B_0 / B_1 > 0$. Also, $Q_0 := V_0 / B_1$, and both Q_0 and α_k have dimensions of charge. In what follows, we sometimes need to distinguish between the two ‘exceptional equations’, (17a) and (17b), and the ‘general equation’, (17c), which is true for $|k| \geq 2$. Here, there are just two exceptional equations because $B(t)$ and $V(t)$ are truncated at the first harmonic: the number of exceptional equations grows linearly with the number of harmonics retained in $B(t)$ and $V(t)$.

There are two approaches to solving equations (17), and we explain these in the following two subsections. In the first, we show an arithmetical solution and in the second, we show how the same solution can be constructed using Bessel functions, and we briefly discuss the asymptotic behaviour of this solution.

4.1 Arithmetical solution

Here is a practical method for solving the difference equations (17) for α_k , $k \in \mathbb{Z}$ and with $\alpha_{-k} = \alpha_k^*$. There should be no free parameters in the solution, even though solving (17) is equivalent to solving the original o.d.e., whose general solution contains one arbitrary constant. However, here we seek only the periodic solution, $q(t)$, to the o.d.e., and not the general solution, $q_c(t)$: only the latter contains an arbitrary constant.

The general solution to (17c), which is of second order, has two arbitrary parameters. One just sets the scale, since, if α_k is a solution, then so is $\lambda\alpha_k$ for any λ . In fact, this scaling is set by either one of (17a), (17b). However, we still need one more relation in order to pin down the second arbitrary parameter. By analogy with the usual procedure for solving Mathieu’s equation [16], this is furnished

by considering the ratio $\rho_k := \alpha_k/\alpha_{k-1}$. For $k \geq 2$, we have

$$\rho_{k+1} = \eta(1 + i\varepsilon k) - \frac{1}{\rho_k} = d_k - \frac{1}{\rho_k},$$

where $d_k := \eta(1 + i\varepsilon k)$. Hence, $\rho_k = 1/(d_k - \rho_{k+1})$, giving the continued fraction expansion

$$\rho_n = \frac{\alpha_n}{\alpha_{n-1}} = \frac{1}{d_n - \frac{1}{d_{n+1} - \frac{1}{d_{n+2} - \dots}}} \quad (18)$$

From equation (18), we can now compute ρ_3 , which depends on η, ε but not on α_k . Then we use equations (17a) and (17b), and equation (17c) with $k = 2$, along with the definition of ρ_3 , to find $\alpha_0, \dots, \alpha_3$. That is, we solve

$$2 \operatorname{Re} \alpha_1 = \eta \alpha_0 - 2Q_0, \quad \alpha_2 = d_1 \alpha_1 - \alpha_0 + Q_0, \quad \alpha_3 = d_2 \alpha_2 - \alpha_1 \quad \text{and} \quad \alpha_3 = \rho_3 \alpha_2 \quad (19)$$

for $\alpha_0, \dots, \alpha_3$, obtaining

$$\alpha_0 = \frac{2Q_0(x+1)}{\eta+2x}, \quad \alpha_1 = w(Q_0 - \alpha_0); \quad (20)$$

then we use the second and third expressions in equation (19) to find α_2, α_3 in terms of α_0, α_1 . Here, $w = (d_2 - \rho_3)/(1 - d_1(d_2 - \rho_3))$ and $x = \operatorname{Re} w$.

Knowing α_2, α_3 , we can now compute α_k for $k \geq 4$ from the general equation — but not in the obvious way, that is, by finding α_4 , followed by α_5 and so on, since iteration in this direction is unstable: the values of α_k so obtained rapidly become inaccurate, even for moderate values of k , and especially for large R . Instead, following section 19.28 in [16], where an analogous problem is solved, we iterate in the reverse direction: we fix a maximum value of k , K , say, and invert the general equation (17) to give $\alpha_{k-1} = d_k \alpha_k - \alpha_{k+1}$. We then use this to find, successively α_{K-j} , $j = 1, \dots, K-2$, each in terms of α_K, α_{K+1} , which are, for the moment, unknown. At stage j , we will have an expression of the form $\alpha_{K-j} = u_j \alpha_K + v_j \alpha_{K+1}$, where $u_j, v_j \in \mathbb{C}$. Now, for $j = K-3$ and $K-2$, we have $\alpha_3 = u_{K-3} \alpha_K + v_{K-3} \alpha_{K+1}$ and $\alpha_2 = u_{K-2} \alpha_K + v_{K-2} \alpha_{K+1}$, and, since α_2 and α_3 are known, we can solve these two equations for α_K and α_{K+1} . With these now known, we can find α_k , $k = 4, \dots, K+1$, and hence $q(t)$ (from equation (16)). In particular, $q(0) \approx \sum_{|k| \leq K+1} \alpha_k$, which we used as our initial condition in the numerical computation of $q(t)$ in section 3.4.

Figure 5 shows a logarithmic plot of the modulus of the first 21 Fourier coefficients so obtained, in the cases $R = 10^7, 10^9$ and $10^{10}\Omega$. For comparison, we compute the mean power $\langle p(R) \rangle$ by (a) $2\omega^2 R \sum_k k^2 |\alpha_k|^2$; (b) by solving the o.d.e. (2) numerically, as was done for Figure 3; and (c) by using the approximate formulae (10), (13), if they apply. The agreement is very good — see Table 2.

Method	$R = 10^7\Omega$	$R = 10^9\Omega$	$R = 10^{10}\Omega$
(a) Sum of Fourier coefficients	0.9652μW	17.80μW	4.132μW
(b) Numerical solution of o.d.e	0.9652μW	17.80μW	4.132μW
(c) Eq. (10) or (13) if valid	0.9652μW	—	4.130μW

Table 2: Comparison of the mean power computed in three different ways, for three different values of R . The first value in row (c) comes from equation (10), the third from (13). Neither formula applies for $R = 10^9\Omega$.

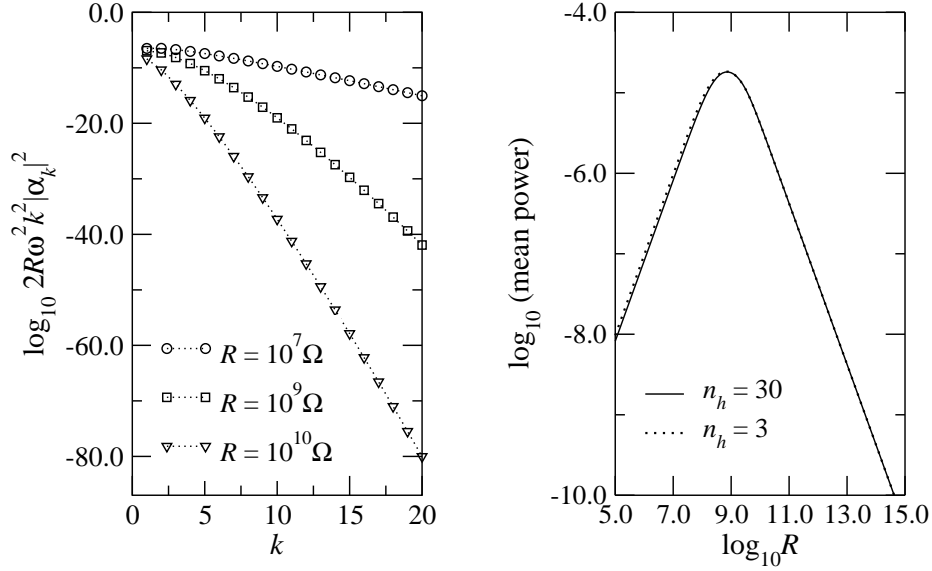


Figure 5: Left: A logarithmic plot of the energy in the k -th harmonic, $\log_{10} 2R\omega^2 k^2 |\alpha_k|^2$, $k = 1, \dots, 20$, computed as described in section 4.1, for $R = 10^7, 10^9$ and $10^{10} \Omega$. Right: Mean power as a function of R computed from $2\omega^2 R \sum_{k=1}^{n_h} k^2 |\alpha_k|^2$, with $n_h = 30$ and $n_h = 3$. Compare with Figure 3.

We now make a practical point. In general, the values of $|\alpha_k|$ decrease very rapidly with k , the more so with increasing R . In fact, to a good approximation, for $R \in [10^5, 10^{15}] \Omega$, we can use

$$\langle p(R, n_h) \rangle := 2\omega^2 R \sum_{k=1}^{n_h} k^2 |\alpha_k|^2, \quad (21)$$

for a small number of harmonics, n_h . For an accurate estimate of the mean power, we use $n_h = 30$. However, even with $n_h = 3$, using equations (19) and (20) to find α_1 , α_2 and α_3 , the largest relative error between $\langle p(R, 3) \rangle$ and $\langle p(R, 30) \rangle$ is about 15%; this largest relative error occurs for $R \in [10^5, 3 \times 10^7]$ and is approximately constant over this range — see Figure 5. For other values of n_h , we find the following maximum relative errors: $n_h = 4$: 6%, $n_h = 5$: 2.5%, $n_h = 7$: 0.3%.

With an algorithm to compute the Fourier coefficients now in place, we can do more however. For instance, we can study the effect of ω on the power output, and we include in Figure 6 a plot of the peak mean power obtained as R varies, as a function of ω . Specifically, we compute the mean power, $\langle p(R, n_h) \rangle$, from (21) with $n_h = 30$, which is large enough to ensure that the error is completely negligible, and then vary R to find the maximum value of the mean power, $\langle p(\omega) \rangle_{pk}$. That is, $\langle p(\omega) \rangle_{pk} := \max_{R>0} \langle p(R, 30) \rangle$. We then denote by $R_{pk}(\omega)$ the value of R for which $\langle p(\omega) \rangle_{pk}$ is obtained. A very strong linear trend is noticeable in both $\langle p(\omega) \rangle_{pk}$ and $R_{pk}(\omega)^{-1}$, and using the data in Figure 6, we find $\langle p(\omega) \rangle_{pk} \approx 2.92\omega \mu\text{W}$ and $R_{pk}(\omega) \approx 4.33/\omega \text{ G}\Omega$. The latter should be compared with equation (14), which predicts that $R_{pk}(\omega) \approx 4.15/\omega \text{ G}\Omega$ for the parameter values in Table 1 — a very good agreement.

The fact that $R_{pk}(\omega)$ is proportional to $1/\omega$ suggests the following way of understanding qualitatively the behaviour of the circuit in Figure 1. If we replace $C(t)$ by a constant capacitance C_{eff} and compute the power transferred to load R , we find that it is a maximum when $R = R_{pk} = 1/(\omega C_{\text{eff}})$. Now, from above, we have that $R_{pk}(\omega) \approx 4.33 \times 10^9/\omega$, suggesting that $C_{\text{eff}} \approx 2.31 \times 10^{-10} \text{ F}$. Looking

now at Figure 2, left, we see that C_{eff} lies between the maximum and minimum values of $C(t)$. It is similar, but not equal to the mean value of $C(t)$, which is about 1.05×10^{-10} F, and it is clear that the actual value of C_{eff} can only be computed from an accurate power computation, such as that carried out here using Fourier series.

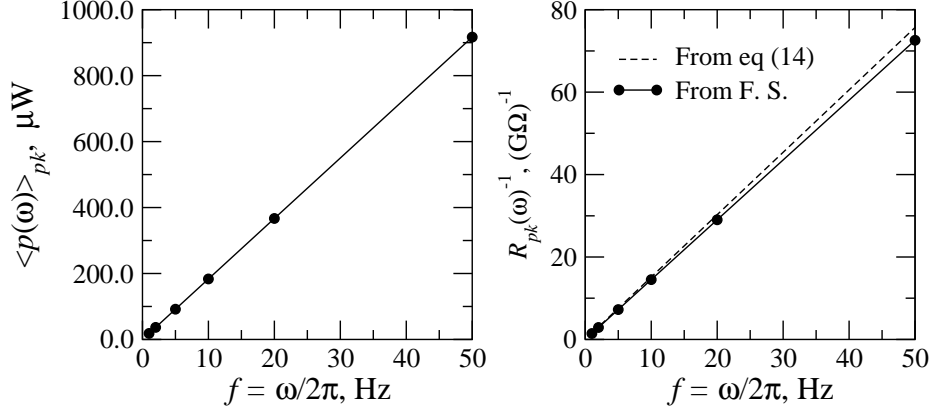


Figure 6: Fourier-series-based power computations. Left: the peak mean power, $\langle p(\omega) \rangle_{pk}$, μW , as a function of frequency $f = \omega/2\pi = 1, 2, 5, 10, 20$ and 50 Hz. Right: $R_{pk}(\omega)^{-1}$, the value of load resistance at which this peak mean power is obtained, plotted for the same values of ω (solid line), alongside the estimate of R_{pk} given in equation (14) (dashed line). The range of R_{pk} itself, as opposed to its reciprocal, is about 14–690 M Ω .

4.2 A solution based on Bessel functions

Along with equations (17), consider also

$$\beta_{k+1} + \beta_{k-1} = \eta(1 + i\varepsilon k)\beta_k, \quad k \in \mathbb{Z} \quad (22)$$

and

$$\gamma_{k+1} + \gamma_{k-1} = \eta(1 - i\varepsilon k)\gamma_k, \quad k \in \mathbb{Z}. \quad (23)$$

The Bessel function of the first kind [16], $J_\nu(z)$, is defined for $\nu, z \in \mathbb{C}$, with ν referred to as the order, and this function obeys

$$J_{\nu+1}(z) + J_{\nu-1}(z) = \frac{2\nu}{z}J_\nu(z). \quad (24)$$

In the light of this, solutions to equation (22) can be expressed in terms of a Bessel function of the appropriate (complex) order. For this to work, we require that $\eta(1 + i\varepsilon k) = 2\nu/z$ for all k , where z is independent of k , and $\nu = k + i\xi$ for $\xi \in \mathbb{R}$. Taking these together, we see that $z\eta(1 + i\varepsilon k) = 2k + 2i\xi$, and so z must be purely imaginary. Hence $\nu = k - i/\varepsilon$ and $z = -2i/\eta\varepsilon$, giving $\beta_k = CW_k$ where $W_k := J_{k-i/\varepsilon}(-2i/\eta\varepsilon)$ and C is an arbitrary constant. Note that $J_\nu(z)$ is bounded as $\text{Re}(\nu) \rightarrow +\infty$, as shown in Appendix II, Property 1. Analogously, for any $k \in \mathbb{Z}$, equation (23) has the solution $\gamma_k = DZ_k$, where D is an arbitrary constant and $Z_k := J_{k+i/\varepsilon}(2i/\eta\varepsilon)$.

Now set $\delta_k = \beta_k$ for $k \geq 1$ and $\delta_k = \gamma_{-k}$ for $k \leq -1$. Then, for $k \geq 2$, we have

$$\delta_{k+1} + \delta_{k-1} = \beta_{k+1} + \beta_{k-1} = \eta(1 + i\varepsilon k)\beta_k = \eta(1 + i\varepsilon k)\delta_k,$$

while, for $k \leq -2$,

$$\delta_{k+1} + \delta_{k-1} = \gamma_{-(k+1)} + \gamma_{-(k-1)} = \gamma_{-k-1} + \gamma_{-k+1} = \eta(1 + i\varepsilon k) \gamma_{-k} = \eta(1 + i\varepsilon k) \delta_k,$$

so that, comparing the last two equations with (17c), we see that, if we set $\alpha_k = \delta_k$ for all $|k| \geq 1$, we obtain a solution to (17c) depending on the complex constants C and D .

Now, Property 2 in Appendix II states that $J_{\nu^*}(z^*) = (J_{\nu}(z))^*$. Hence, setting $D = C^*$, for all $k \geq 1$, we have

$$\alpha_k^* = \beta_k^* = C^* W_k^* = C^* (J_{k-i/\varepsilon}(-2i/\eta\varepsilon))^* = D J_{k+i/\varepsilon}(2i/\eta\varepsilon) = D Z_k = \gamma_k = \alpha_{-k} \quad (25)$$

so that $\alpha_k^* = \alpha_{-k}$ for all $k \neq 0$. So, if we require $q(t)$ to be real, we are left with only one free parameter $C \in \mathbb{C}$.

To compute C , we go back to equations (17a), (17b). Solving these for α_0 gives

$$\alpha_0 = \frac{C W_1 + C^* W_1^* + 2Q_0}{\eta} = \eta(1 + i\varepsilon) C W_1 - C W_2 + Q_0, \quad (26)$$

where we have used $\alpha_i = C W_i$ for $i = 1, 2$. The right-hand equality can be rewritten in the form $z_1 C + z_2 C^* = r$, where $z_1, z_2, C \in \mathbb{C}$ and $r \in \mathbb{R}$. Specifically, $z_1 = W_1(1 - \eta^2(1 + i\varepsilon))/\eta + W_2$, $z_2 = W_1^*/\eta$ and $r = Q_0(1 - 2/\eta)$. By considering $z_1 C + z_2 C^* = r$ and its complex conjugate, we can solve for C to obtain $C = r(z_1^* - z_2)/\Delta$, where $\Delta = |z_1|^2 - |z_2|^2$. Numerical evidence indicates that $\Delta \in (0, 1)$ for all $R > 0$, so C exists for all positive R .

The expression $\alpha_k = C J_{k-i/\varepsilon}(-2i/\eta\varepsilon)$, $k \geq 1$, with α_0 being given by (26), is in principle good for any values of the parameters. In practice, however, the method for computing α_k in Section 4.1 is often useful, especially for small R (leading to small $\varepsilon = \omega R/B_0$, which requires the evaluation of $J_{k-i/\varepsilon}(z)$ for small ε — algorithms to do this tend to be slow, especially when $|k - i/\varepsilon| \approx |z|$).

One advantage of expressing the Fourier coefficients in terms of Bessel functions is that we immediately see from our expression for α_k , along with (31) in Appendix II, that

$$|\alpha_k| \sim \left(\frac{e}{\eta\varepsilon}\right)^k \frac{1}{k^{k+\frac{1}{2}}},$$

so clearly the Fourier series for $q(t)$ converges for all non-zero ε, η .

5 Conclusions and further work

We have studied the periodically-excited triboelectric nanogenerator (TENG) from a mathematical viewpoint. Our main aim has been to derive expressions for the mean power as a function of load resistance R and excitation frequency ω , although as a by-product, we also compute the current, from which other quantities of interest can be derived.

The TENG has a single state variable, the charge, $q(t)$, and the time evolution of $q(t)$ is described by the linear, first-order, non-autonomous o.d.e. in equation (2). This has a periodically-varying coefficient, the reciprocal capacitance $B(t)$, which makes analysis of the problem less straightforward than, say, the piezoelectric device discussed in [10], the o.d.e. for which, while still non-autonomous, has constant coefficients.

After proving that the o.d.e. (2) has a unique periodic attractor, we derive perturbation series for $q(t)$ in the cases of small and large R , equations (10) and (13) respectively. We give general expressions for the first few coefficients in these series before using them to estimate the current, $i(t) = \dot{q}(t)$, and the mean power, $R \times [\text{mean squared current over one period}]$. Comparison with numerics shows these expressions to be good for all R except $R \in [10^8, 3 \times 10^9]\Omega$ (approximately), these values of R being neither ‘small’ nor ‘large’ in the context of this problem. However, by using a simple argument based on the intersection of straight lines, the two perturbation series can be used to estimate R_{pk} , the value of R that maximises the mean power, and this approach results in a simple expression, equation (14), for $R_{pk}(\omega)$.

Since the o.d.e. has a unique periodic solution $q(t)$, we then discuss its Fourier expansion. We give two procedures to find the Fourier coefficients, α_k , for k as large as desired. The first is an algorithm to find α_k , which requires only simple computing machinery, and the second is an expression for α_k in terms of Bessel functions of the first kind, $J_\nu(z)$. From α_k , the mean power, for any R and ω , can be computed to any degree of precision, as can $q(t)$ and $i(t)$ — from the latter, the peak current and peak power can then be found if desired. One important aspect of the connection with Bessel functions is that we can deduce the behaviour of α_k for large k .

Our chief interest has been the mean power as a function of R and ω and we discuss how this may be estimated by a single expression, valid for *all* R . We propose two possibilities. The first is heuristic and comes from an observation about the two series, equations (10) and (13): we show that if these series are both expansions of the same rational function, then we can compute an approximation to this function explicitly — see equation (15). This estimate is simple to use but entirely heuristic, although it does compare favourably with the exact result.

The second possibility comes from our study of the Fourier coefficients in terms of Bessel functions, which shows that they decrease in magnitude rapidly (as $1/k!$ in fact) with increasing index k . In practice, even the first three coefficients are enough to give a reasonable power estimate (relative error $\leq 15\%$) for all R .

Clearly, the power output also depends on other parameters in the problem, for example the thickness x_1, x_2 of the dielectrics, the excitation amplitude z_0 and the triboelectric charge density σ_T . A study of the effects of these parameters and others has recently been published in [17].

This work raises some interesting questions for further investigation. For example, in the TENG context, the fundamental frequencies of $B(t)$ and $V(t)$ have to be the same. What can we say about solutions to o.d.e.s like (2) where this is not the case? What more can we say about the convergence of the perturbation series? Can we say anything about the behaviour of the modulus of the Fourier coefficients in the case where $B(t)$ and/or $V(t)$ are not approximated as truncated Fourier series? What can we say in the case of a load that is not purely resistive?

References

- [1] R.D.I.G. Dharmasena, K.D.G.I. Jayawardena, C.A. Mills, J.H.B. Deane, R.A. Dorey and S.R.P. Silva, *Triboelectric Nanogenerators: Providing a Fundamental Framework*, **Energy & Environmental Science**, vol. 10, pp 1801–1811 (13 July 2017) doi.org/10.1039/C7EE01139C
- [2] Y. Wang, Y. Yang and Z.L. Wang, *Triboelectric nanogenerators as flexible power sources*, **npj Flexible Electronics**, vol. 1, article 10 (2017)

- [3] Z.L. Wang, *Triboelectric nanogenerators as new energy technology and self-powered sensors – Principles, problems and perspectives*, **Faraday Discussions**, vol. 176, pp 447–458 (2014) doi.org/10.1039/C4FD00159A
- [4] R.D.I.G. Dharmasena, K.D.G.I. Jayawardena, C.A. Mills, R.A. Dorey, S.R.P. Silva, *A unified theoretical model for Triboelectric Nanogenerators*, **Nano Energy**, vol. 48, pp 391–400 (2018)
- [5] J. Chen and Z.L. Wang, *Reviving Vibration Energy Harvesting and Self-Powered Sensing by a Triboelectric Nanogenerator*, **Joule**, vol. 1, pp 480–521 (2017) doi.org/10.1016/j.joule.2017.09.004
- [6] Z.L. Wang, J. Chen Z.L. Wang and L. Lin, *Progress in triboelectric nanogenerators as a new energy technology and self-powered sensors*, **Energy & Environmental Science**, vol. 8, pp 2250–2282 (2015) doi.org/10.1039/C5EE01532D
- [7] Z.L. Wang, *Triboelectric Nanogenerators as New Energy Technology for Self-Powered Systems and as Active Mechanical and Chemical Sensors*, **ACS Nano**, vol. 7(11), pp 9533–9557 (2013) doi.org/10.1021/nn404614z
- [8] S. Niu, S. Wang, L. Lin, Y. Liu, Y.S. Zhou, Y. Hu and Z.L. Wang, *Standards and figure-of-merits for quantifying the performance of triboelectric nanogenerators*, **Energy & Environmental Science**, vol. 6, pp 3576–3583 (2013) doi.org/10.1039/C3EE42571A
- [9] Y. Zi, S. Niu, J. Wang, Z. Wen, W. Tang and Z.L. Wang, *Standards and figure-of-merits for quantifying the performance of triboelectric nanogenerators*, **Nature Communications**, vol. 6, p 8376 (2015) doi.org/10.1038/ncomms9376
- [10] Y. Zhang, B. Lu, C. Lü and X. Feng, *Theory of energy harvesting from heartbeat including the effects of pleural cavity and respiration*, **Proceedings of the Royal Society A** vol. 473, 2214 (2017) doi.org/10.1098/rspa.2017.0615
- [11] S. Niu and Z.L. Wang, *Theoretical systems of triboelectric nanogenerators*, **Nano Energy** vol. 14, pp 161–192 (2015) doi.org/10.1016/j.nanoen.2014.11.034
- [12] S. Haykin, *Communication systems*, **John Wiley & sons**, ISBN 0471 57176 8 (1994)
- [13] H.T.H. Piaggio, *An elementary treatise on differential equations and their applications* **Bell’s Mathematical Series**, **G. Bell and sons Ltd, London**, (1944)
- [14] Documentation for the Livermore Solver for Ordinary Differential Equations — <https://computation.llnl.gov/casc/nsde/pubs/u113855.pdf>
- [15] C.J. Tranter, *Bessel functions with some physical applications*, **The English Universities Press Ltd.**, ISBN 0340 04959 6 (1968)
- [16] M. Abramowitz and I.A. Stegun, *Handbook of Mathematical Functions*, **Dover Publications Inc., New York**, ISBN 0486 61272 4 (1972)
- [17] R.D.I.G. Dharmasena, J.H.B. Deane and S.R.P. Silva, *Nature of Power Generation and Output Optimisation of Triboelectric Nanogenerators*, **Advanced Energy Materials**, (in press) doi:10.1002/aenm.201802190

Appendix I — derivation of $I(x)$

This appendix gives the mathematical part of the derivation of the function $I(x)$ that features in the o.d.e. studied in this paper, and it is included for the sake of completeness. The context is a device known as a triboelectric generator, consisting of a pair of parallel rectangular plates whose sides are of length l and w .

The definition of $I(x)$ is the following indefinite integral:

$$I(x) := \int \arctan \left(\frac{l/w}{2(x/w)\sqrt{4(x/w)^2 + (l/w)^2 + 1}} \right) dx.$$

It arises as a consequence of Gauss' law, and we have taken the integral directly from [1], which should be consulted for further details. Setting $\alpha = l/w$ and substituting $y = x/w$, this becomes

$$I(y) = w \int \arctan \left(\frac{\alpha}{2y\sqrt{4y^2 + \alpha^2 + 1}} \right) dy. \quad (27)$$

Perhaps surprisingly, this integral can be expressed in closed form for all $\alpha > 0$, provided that $x > 0$. The first step to showing this is to multiply the integrand by 1 and integrate by parts, giving

$$\frac{I}{w} = y \arctan \left(\frac{\alpha}{2y\sqrt{4y^2 + \alpha^2 + 1}} \right) - \int y \frac{d}{dy} \arctan \left(\frac{\alpha}{2y\sqrt{4y^2 + \alpha^2 + 1}} \right) dy.$$

We then use

$$\frac{d}{dy} \arctan \left(\frac{1}{g(y)} \right) = \frac{-g'(y)}{1 + g^2(y)},$$

and with $g(y) = (2y/\alpha)\sqrt{4y^2 + \alpha^2 + 1}$, we find

$$\frac{I}{w} = y \arctan \left(\frac{\alpha}{2y\sqrt{4y^2 + \alpha^2 + 1}} \right) + 2\alpha \int \frac{y(8y^2 + \alpha^2 + 1)}{\sqrt{4y^2 + \alpha^2 + 1} [4y^2(4y^2 + \alpha^2 + 1) + \alpha^2]} dy.$$

Now define

$$I_1 = \int \frac{y(8y^2 + \alpha^2 + 1)}{\sqrt{4y^2 + \alpha^2 + 1} [4y^2(4y^2 + \alpha^2 + 1) + \alpha^2]} dy$$

and substitute $u^2 = 4y^2 + \alpha^2 + 1$. This gives

$$I_1 = \int \frac{y(2u^2 - \alpha^2 - 1)}{u(4u^2y^2 + \alpha^2)} \frac{u}{4y} du = \frac{1}{4} \int \frac{2u^2 - \alpha^2 - 1}{4u^2y^2 + \alpha^2} du,$$

and using $4y^2 = u^2 - \alpha^2 - 1$, we find

$$\begin{aligned} I_1 &= \frac{1}{4} \int \frac{2u^2 - \alpha^2 - 1}{u^2(u^2 - \alpha^2 - 1) + \alpha^2} du = \frac{1}{4} \int \frac{2u^2 - \alpha^2 - 1}{(u^2 - \alpha^2)(u^2 - 1)} du \\ &= \frac{1}{4} \int \frac{(u^2 - \alpha^2) + (u^2 - 1)}{(u^2 - \alpha^2)(u^2 - 1)} du = \frac{1}{4} \int \frac{1}{u^2 - 1} + \frac{1}{u^2 - \alpha^2} du. \end{aligned}$$

Expressing both these terms in partial fractions, we then obtain

$$I_1 = \frac{1}{8} \ln \frac{u-1}{u+1} + \frac{1}{8\alpha} \ln \frac{u-\alpha}{u+\alpha}.$$

Hence, finally, we have

$$I(x) = x \arctan \frac{\alpha w}{2xu} + \frac{w}{4} \left(\alpha \ln \frac{u-1}{u+1} + \ln \frac{u-\alpha}{u+\alpha} \right), \quad (28)$$

where $u = \sqrt{4(x/w)^2 + \alpha^2 + 1}$.

Points to note:

- The expressions for $I(x)$ and I_0 are unchanged if l and w are swapped (which also replaces $\alpha = l/w$ with α^{-1}). This is, of course, exactly as it should be: it cannot matter which way round we label the sides of the rectangular plates.
- Since both $\arctan x > 0$ and $\alpha/(2x\sqrt{4x^2 + \alpha^2 + 1}) > 0$ for $x > 0$, $I(x)$ is the integral of a strictly positive function, and so $I(x)$ is a monotonically increasing function of $x > 0$. Hence, $G(t)$ as defined in equation (1) is always positive provided only that $x_1 + x_2 > 0$; and so $B(t) = G(t)/A > 0$ for all t .

We shall also need $I_0 = \lim_{x \rightarrow 0} I(x)$, which is

$$I_0 = \frac{\alpha w}{4} \ln \left(\frac{\alpha^2 + 2 - 2\sqrt{\alpha^2 + 1}}{\alpha^2} \right) + \frac{w}{4} \ln \left(2\alpha^2 + 1 - 2\alpha\sqrt{\alpha^2 + 1} \right).$$

When $\alpha = 1$, this gives $I_0 = (w/2) \ln(3 - 2\sqrt{2}) \approx -0.881374w$.

Appendix II — properties of $J_\nu(z)$

Property 1. Fix $u \neq 0 \in \mathbb{R}$ and $z \in \mathbb{C}$. Then, as $k \rightarrow \infty$, $|J_{k+iu}(z)| \rightarrow 0$.

Proof. Equations (29) and (30) below are taken from [16], [15]. Equations (29) and (30), and all the asymptotic expansions in this proof, have an error term which multiplies the right-hand sides by a factor $(1 + O(|\nu|^{-1}))$. We start from the asymptotic expansion

$$J_\nu(z) \sim \frac{1}{\Gamma(\nu+1)} \left(\frac{z}{2} \right)^\nu. \quad (29)$$

The latter is valid for fixed $z \in \mathbb{C}$ and complex ν with $|\nu| \gg |z|$. Stirling's approximation for large $|\nu|$ is

$$\Gamma(\nu+1) \sim \sqrt{2\pi\nu} \left(\frac{\nu}{e} \right)^\nu. \quad (30)$$

We put $\nu = k + iu$, where $k \in \mathbb{Z}$, and set $\theta = \arg \nu$. With these definitions, applying Stirling's approximation to equation (29), we obtain

$$J_\nu(z) \sim \frac{1}{\sqrt{2\pi\nu}} \left(\frac{ze}{2\nu} \right)^\nu = \frac{1}{\sqrt{2\pi}} \left(\frac{ze}{2} \right)^{iu} \times e^{u\theta} e^{-iu \ln |\nu|} e^{-i\theta(k+\frac{1}{2})} \left(\frac{ze}{2} \right)^k \frac{1}{|\nu|^{k+\frac{1}{2}}}.$$

Only terms to the right of the \times symbol depend on k . Furthermore, we can replace $e^{u\theta}$ with unity, since u is fixed, so $\theta = \lim_{k \rightarrow \infty} \arg(k + iu) = 0$. Hence, taking the modulus,

$$|J_{k+iu}(z)| \sim C \left(\frac{|z|e}{2} \right)^k \frac{1}{k^{k+\frac{1}{2}}}, \quad (31)$$

where $C > 0$ is independent of k . The property is then established by letting $k \rightarrow \infty$. \square

Property 2. For $\nu, z \in \mathbb{C}$, $J_{\nu^*}(z^*) = (J_{\nu}(z))^*$.

Proof. This follows from the series representation [16] of the Bessel function

$$J_{\nu}(z) = \sum_{m=0}^{\infty} \frac{(-1)^m}{m! \Gamma(m + \nu + 1)} \left(\frac{z}{2} \right)^{2m+\nu}$$

along with the property that $\Gamma(z^*) = (\Gamma(z))^*$ of the Gamma function [16] and the fact that $(z^*)^{\alpha^*} = (z^{\alpha})^*$. The latter can be seen by writing $z = re^{i\theta}$, $\alpha = a + ib$ and expanding. \square